THE JOURNAL OF BIOLOGICAL CHEMISTRY VOL. 282, NO. 2, pp. 1039–1050, January 12, 2007

Execution of Macrophage Apoptosis by PE_PGRS33 of *Mycobacterium tuberculosis* Is Mediated by Toll-like Receptor 2-dependent Release of Tumor Necrosis Factor-α*

Received for publication, May 8, 2006, and in revised form, October 30, 2006 Published, JBC Papers in Press, November 9, 2006, DOI 10.1074/jbc.M604379200

Sanchita Basu[‡1], Sushil Kumar Pathak[‡1,2], Anirban Banerjee[‡], Shresh Pathak[‡], Asima Bhattacharyya[‡3], Zhenhua Yang[§], Sarah Talarico[§], Manikuntala Kundu[‡], and Joyoti Basu[‡4]

From the [‡]Department of Chemistry, Bose Institute, 93/1 Acharya Prafulla Chandra Road, Kolkata 700009, India and the [§]Department of Epidemiology, School of Public Health, University of Michigan, Ann Arbor, Michigan 48105

Combating tuberculosis requires a detailed understanding of how mycobacterial effectors modulate the host immune response. The role of the multigene PE family of proteins unique to mycobacteria in the pathogenesis of tuberculosis is still poorly understood, although certain PE_PGRS genes have been linked to virulence. Tumor necrosis factor-α (TNF-α) is essential for successfully combating tuberculosis. In this study we provide evidence that PE_PGRS33, a surface exposed protein, elicits TNF-α release from macrophages in a TLR2 (Toll-like receptor 2)-dependent manner. ASK1 (apoptosis signal-regulating kinase 1) is activated downstream of TLR2. ASK1 activates the MAPKs p38 and JNK. PE_PGRS33-induced signaling leads to enhanced expression of *TNF-α* and TNF receptor I (*TNFRI*) genes. *Mycobacterium smegmatis* expressing PE_PGRS33 elicits the same effects as purified PE_PGRS33. TNF-α release occurs even when internalization of the bacteria is blocked by cytochalasin D, suggesting that interaction of PE_PGRS33 with TLR2 is sufficient to trigger the effects described. Release of TNF-α plays the determining role in triggering apoptosis in macrophages challenged with PE_PGRS33. The death receptor-dependent signals are amplified through classical caspase 8-dependent mitochondrial release of cytochrome *c*, leading to the activation of caspases 9 and 3. An important aspect of our findings is that deletions within the PGRS domain (simulating those occurring in clinical strains) attenuate the TNF-α-inducing ability of PE_PGRS33. These results provide the first evidence that variations in the polymorphic repeats of the PGRS domain modulate the innate immune response.

Containing infection by microbial pathogens involves both innate and adaptive arms of the host immune response. Tumor necrosis factor-α is a pleiotropic cytokine that plays an important role in determining the outcome of tuberculosis by inducing a range of cytokines and chemokines, as well as apoptosis (1). It is widely accepted that TNF-α[5] is essential for the maintenance of the granuloma and the control of tuberculosis (2). Hosts with a deficiency in TNF-α or its receptors are susceptible to mycobacterial infection (3–8). TNF-α controls both the innate and the adaptive arms of the immune response against tuberculosis. Recent studies have shown that $TNF^{-/-}$ mice undergo an uncontrolled expansion of CD4 and CD8 T cells (9). Patients receiving anti-TNF therapy for chronic inflammatory diseases are susceptible to tuberculosis, providing evidence that TNF-α has a role in controlling tuberculosis in humans (10–12). Considering its central role in defining the course of tuberculosis infection, it is important to understand how the microbe regulates TNF-α induction in the host and how this is related to the regulation of key events such as the induction of proinflammatory cytokines/chemokines.

Because *Mycobacterium tuberculosis* resides in macrophages, the course of the infection rests on the outcome of the interaction between the bacterium and the host macrophages. Paradoxically, macrophages provide an intracellular niche for the invading pathogen and also restrict the pathogen by a variety of mechanisms. This duality of function has been analyzed in a recent report by Leemans *et al.* (13) who have suggested that the bacterium resides in resting macrophages, whereas activated macrophages deliver the antimicrobicidal arsenal required to limit the pathogen. Apoptosis of resting macrophages is likely to be a part of the immune defense mechanism. Mycobacteria-induced apoptosis of infected macrophages releases mycobacterial antigen-containing apoptotic vesicles. These vesicles are engulfed by dendritic cells, which process the antigenic cargo for subsequent presentation to CD8 T cells (14). Several lines of evidence suggest that TNF-α plays a critical role

* This work was supported in part by a grant from the Department of Science and Technology, Government of India (to J. B.). The costs of publication of this article were defrayed in part by the payment of page charges. This article must therefore be hereby marked "*advertisement*" in accordance with 18 U.S.C. Section 1734 solely to indicate this fact.

[1] Both authors contributed equally to this work.

[2] Supported by a fellowship from Council of Scientific and Industrial Research, Government of India.

[3] Present address: Dept. of Medicine, Division of Gastroenterology and Hepatology, University of Virginia Health System, Charlottesville, VA 22903.

[4] To whom correspondence should be addressed. Fax: 913323506790; E-mail: joyoti@vsnl.com.

[5] The abbreviations used are: TNF-α, tumor necrosis factor-α; CCCP, carbonyl cyanide *m*-chlorophenylhydrazone; cyt *c*, cytochrome *c*; t-Bid, truncated Bid; Z-DEVD-FMK, benzyloxycarbonyl-Asp(OCH_3)-Glu(OCH_3)-Val-Asp(OCH_3)-fluoromethyl ketone; Z-LEHD-FMK, benzyloxycarbonyl-Leu-Glu(OMe)-His-Asp(OMe)-CH_2F; Z-IETD-FMK, benzyloxycarbonyl-Ile-Glu(OMe)-Thr-Asp(OMe)-fluoromethyl ketone; $DiOC_6$, 3,3′-dihexyloxacarbocyanine; MAPK, mitogen-activated protein kinase; MDM, monocyte-derived macrophages; PRRs, pattern recognition receptors; PBS, phosphate-buffered saline; PIPES, 1,4-piperazinediethanesulfonic acid; PVDF, polyvinylidene difluoride; CHAPS, 3-[(3-cholamidopropyl)dimethyl ammonio]-1-propanesulfonic acid; RT, reverse transcription; NTA, nitrilotriacetic acid; ELISA, enzyme-linked immunosorbent assay; LPS, lipopolysaccharide; BSA, bovine serum albumin; FBS, fetal bovine serum; JNK, c-Jun N-terminal kinase; IL, interleukin; TLR, Toll-like receptor.

in modulating apoptosis associated with *M. tuberculosis* infection. Inactivation of TNF-α is linked to the ability of *M. tuberculosis* to evade apoptosis of host macrophages (15, 16). Based on the above, it is important to dissect the repertoire of mycobacterial molecules delivering TNF-α-dependent pro-apoptotic signals to macrophages, and to understand how mycobacteria may have developed mechanisms to suppress these signals.

Eight percent of the coding sequence of the *M. tuberculosis* genome is dedicated to members of the unrelated PE and PPE gene families, characterized by the presence of N-terminal Pro-Glu and Pro-Pro-Glu motifs in the respective families (17). Linkage of glycine-rich sequences encoded by polymorphic GC-rich repetitive sequences (PGRS) to the C-terminal ends of the PE domains is characteristic of the PE_PGRS family of proteins. Several PE_PGRS proteins are localized on the extracellular surface of *M. tuberculosis* (18, 19). One such protein is PE_PGRS33 (encoded by the open reading frame Rv1818c of *M. tuberculosis* H37Rv) (20). A role of certain PE_PGRS proteins in virulence was suggested by gene inactivation studies in *Mycobacterium marinum.* Inactivation of two PE_PGRS genes resulted in a replication defect in macrophages and decreased survival in granulomas (21). Global expression profiles have shown that the PE/PPE genes are not regulated as one group, but rather they show variable expression patterns under different environmental conditions likely dictated by different regulatory circuits (22). The PE/PPE proteins are therefore likely to fulfill diverse functions in the biology of *M. tuberculosis*.

The host response to infection is initiated by the early response of the innate immune system to an array of conserved pathogen-associated molecular patterns. It is therefore likely that differences in the virulence of *M. tuberculosis* could relate to differences in this early response. The Toll-like receptors (TLRs) are evolutionarily conserved pattern recognition receptors (PRRs) that recognize pathogen-associated molecular patterns (23). The diversity of the innate immune response to pathogens is to a large extent generated by the diversity of signaling triggered by the TLRs and their adapters. Given that pathogenic mycobacteria infect professional phagocytes, there has understandably been considerable interest in deciphering how TLR-mediated signals can control the innate immune response to mycobacteria. TLR2-deficient mice have been reported to be susceptible to *M. tuberculosis* infection (24), particularly in a high dose aerosol challenge model (25).

The complementary approaches of using either individual molecules or the intact bacterium modified in expression of a particular molecule to study effects on host cell signaling in the context of innate immunity contribute toward detailed understanding of immune signaling in response to mycobacterial infection. In this study we have used both approaches to evaluate how one member of the unique PE_PGRS family of *M. tuberculosis* proteins, namely PE_PGRS33, regulates macrophage signaling. We provide evidence that the induction of TNF-α by PE_PGRS33 occurs in a TLR2-dependent manner and leads to consequent macrophage apoptosis. The apoptotic signals generated by PE_PGRS33-induced TNF-α release are amplified in a mitochondria-dependent pathway. The PGRS domain is responsible for mediating TNF-α release. The PGRS domain of PE_PGRS33 shows a large number of variations in clinical strains (26). The most important results of our study reflect that the deletion of some of the PGRS repeats within this domain (simulating the deletions that exist in putative PE_PGRS33 proteins from clinical isolates of *M. tuberculosis*) impact the TNF-α-inducing ability of the respective proteins. These findings are of potential clinical relevance and suggest that polymorphisms in the PGRS domain help clinical strains of *M. tuberculosis* modulate the release of TNF-α from macrophages. These modulatory effects could potentially regulate the clinical course of the disease.

EXPERIMENTAL PROCEDURES

Reagents—Antibodies against total and phospho-specific MAPKs cleaved caspase 3, caspase 8, and caspase 9 were purchased from Cell Signaling Technology, Beverly, MA. Antibodies against ASK1, Bid, cyt *c*, β-actin, and protein A/G (plus)-agarose were purchased from Santa Cruz Biotechnology Inc., Santa Cruz, CA. SB203580, U0126, SP600125, Z-DEVD-FMK, Z-LEHD-FMK, Z-IETD-FMK, and protease inhibitors were from EMD Biosciences, San Diego 3,3′-Dihexyloxacarbocyanine ($DiOC_6$) and Alexa-488-conjugated anti-rabbit IgG were obtained from Molecular Probes Inc., Eugene, OR. *Escherichia coli* lipopolysaccharide (LPS) and polymyxin B resin were from Sigma. Annexin-fluos, Pefabloc, and protease inhibitor mixture were purchased from Roche Applied Science. Neutralizing TLR-4 antibody (HTA 125) was purchased from Imgenex Biotech, Bhubaneswar, India. Neutralizing anti-TLR2 antibody was a generous gift from Carsten Kirschning, Institute of Medical Microbiology, Immunology, and Hygiene, Technical University of Munich.

Plasmid Constructs—Wild type and dominant-negative murine TLR2, as well as murine TLR4, have been described earlier (27). cDNA of human TLR2 was obtained by RT-PCR from a total RNA preparation from THP-1 cells using the sense and antisense primers pairs 5′-ATAAAGCTTATGCCACATACTTTGTGG-3′ and 5′-ATGGATCCCTAGGACTTTATCGCAGCT-3′, respectively. The resulting PCR product was cloned between the HindIII and BamHI sites (underlined) of pFLAG-CMV-6a. Human TLR4 was similarly reverse-transcribed using the sense and antisense primers 5′-ATGGATCCGCATGGAGCTGAATTTCTA-3′ and 5′-ATAAAGCTTCTAAGATGTTGCTTCCTG-3′, respectively and cloned between the BamHI and HindIII sites (underscored) of pcDNA3.1. Hemagglutinin-tagged wild type ASK1 (ASK1, WT) and a catalytically inactive mutant (K709M) of ASK1 (ASK1, KM) were obtained from Hidenori Ichijo, Graduate School of Pharmaceutical Sciences, The University of Tokyo, Japan. FLAG-tagged p38 and its dominant-negative mutant (p38 (agf)), as well as FLAG-tagged JNK and its dominant-negative mutant (JNK(apf)) were obtained from Roger Davis, University of Massachusetts Medical School, Worcester, MA. Cells were routinely transfected using FuGENE 6 (Roche Applied Science) according to the manufacturer's instructions. β-Galactosidase reporter plasmid was used to normalize transfection efficiencies.

Culture of the Murine Macrophage Cell Line RAW 264.7 and Human Embryonic Kidney Cell Line HEK293—The murine macrophage cell line RAW 264.7 and the human embryonic

TABLE 1
Primers used for the generation of deletion constructs of PE_PGRS33

Antisense primer for 1st fragment	Sense primer for 2nd fragment	Mutation
5′-ATGGTACCGCCGAACCCTGCGGTG-3′	5-ATGGTACCGGGGCCGGCGGGGCCG-3′	Δ(Gly-184 to Gly-213)
5′-ATGGTACCGGCGCCGTAGAGCAGCCC-3′	5′-ATGGTACCGGCGGGGCCGGCGGAG-3′	Δ(Gly-196 to Asp-243)
5′-ATGGTACCGAGTCCGCCGACGCCG-3′	5′-ATGGTACCATCGGATTGGTCGGGAAC-3′	Δ(Leu-237 to Gly-327)
5′-ATGGTACCGGCGTTGCCGCCCGCCC-3′	5′-ATGGTACCGGCCTTCTGTTTGGTACC-3′	Δ(Gly-372 to Ala-403)

kidney cell line HEK293 were obtained from the National Center for Cell Science, Pune, India. RAW 264.7 was maintained in Dulbecco's modified Eagle's medium supplemented with 10% heat-inactivated fetal bovine serum (FBS), 100 units/ml penicillin, and 100 μg/ml streptomycin in a humidified atmosphere containing 5% CO_2. Dishes were washed to remove nonadherent cells. Adherent cells were ≥95% viable as determined by trypan blue dye exclusion. HEK293 cells were grown under similar conditions in modified Eagle's medium supplemented with 10% heat-inactivated FBS, 100 units/ml penicillin, and 100 μg/ml streptomycin.

Cloning and Expression of PE_PGRS Genes—The *PE_PGRS33* gene (Rv1818c) was amplified by PCR using genomic DNA of *M. tuberculosis* H37Rv (kind gift from Jaya Tyagi, All India Institute of Medical Sciences, New Delhi) as template and the primers 5′-ATGGATCCATGTCATTTGTGGTCACGA-3′ (sense) (primer A) and 5′-ATGAATCCCTACGGTAACCCGTTCATC-3′ (antisense) (primer B) with BamHI and EcoRI sites (underscored), respectively, and cloned between asymmetric BamHI and EcoRI sites in the vector pET28a$^+$ (Novagen) for expression. The resulting plasmid is designated pJSK33. The gene encoding the PE domain (amino acid residues 1–140) of the same protein was amplified by PCR using the sense primer given above and the antisense primer 5′-ATGAATTCCTAGCCGATCAAGATTCCC-3′, and cloned between the BamHI and EcoRI sites of pET 28a$^+$ to generate pJSK34. The genes encoding *PE_PGRS62* (Rv3812) and *PE_PGRS48* (Rv2853) were amplified by PCR using the primer pairs 5′-TAGGATCCATGTCGTTCGTGGTCACAGT-3′ (sense) and 5′-AATGAATTCTAAGCCGCCGGTTTGATT-3′ (antisense) for *PE_PGRS62* and 5′-TAGGATCCATGTTGTATGTAGTTGCG-3′ (sense) and 5′-TTAGAATTCAGCCGGGCTGCCCGGGGT-3′ (antisense) for *PE_PGRS48*. The resulting PCR products were cloned between the BamHI and EcoRI sites of pET28a$^+$ to generate pJSK35 and pJSK36 for PE_PGRS62 and PE_PGRS48, respectively. For point mutations and deletion constructs Δ(Gly-217 to Gly-219), Δ(Gly-227 to Gly-229), Δ(Gly-186 to Ala-188), and Δ(Ala-198 to Gly-203), of *PE_PGRS33*, site-directed mutagenesis was carried out by overlap extension PCR using appropriate primers and pJSK33 as template. Other deletion constructs were obtained by two-step PCR and subsequent cloning between the BamHI and EcoRI sites of pET28a. The first PCR product was obtained using the sense primer 5′-ATGGATCCATGTCATTTGTGGTCACGA-3′ and the antisense primers shown in Table 1. The second PCR product was obtained using the antisense primer 5′-ATGAATTCCTACGGTAACCCGTTCATC-3′ and the sense primers shown in Table 1. SA-440 and SA455 variants of PE_PGRS33 (described under Fig. 1) were PCR-amplified using primers described by Talarico *et al.* (26) and genomic DNA of the respective clinical isolates (26) and cloned in pUC19. A second round of PCR was performed using the respective pUC19 constructs and primer pairs A and B, followed by cloning in pET28a$^+$ as described above. All constructs were verified by sequencing of both strands.

Induction of PE_PGRS33 from *E. coli* BL21 (DE3)/pJSK33 was carried out at 37 °C for 4 h with isopropyl thio-β-D-galactoside (250 μM). Cells were harvested, and the cell pellet was resuspended and lysed with Bugbuster HT (Novagen) to which 0.5 mM EDTA and 100 μM Pefabloc was added. Hexa-His-tagged PE-PGRS33 was purified from the soluble fraction by chromatography on Ni^{2+}-NTA-agarose (Qiagen). All experiments were carried out with the purified PE-PGRS33 produced in *E. coli* unless otherwise stated. For expression of variant PE_PGRS proteins, *E. coli* strains Rosetta (Novagen) and C41(DE3) (Avedis, France) were also used. Variant PE_PGRS proteins were purified by chromatography on Ni^{2+}-NTA affinity chromatography.

Cloning and Expression of PE_PGRS33 in HEK293—To generate a Myc-His epitope tag in pcDNA3.1 (−)(Invitrogen), the Myc-His epitope present in pBAD-Myc-HisB (Invitrogen) was amplified using the sense and antisense primers 5′-CGGGATCCGAACAAAAACTCATCT-3′ and 5′-CCCAAGCTTAAGCTGGAGACCGTT-3′, respectively. The resulting PCR product was cloned between the BamHI and HindIII sites (underlined) of pcDNA3.1(−) to generate the vector pcDNA3.1-Myc-His. *PE_PGRS33* was amplified by PCR using the primer pairs 5′-TGC**TCTAGA**ATGTCATTTGTGGTCACGA-3′ (sense) and 5′-CG**GAATTC**ATCGGTAACCCGTTCATCC-3′ (antisense). The resulting PCR product was cloned between the XbaI and EcoR1 sites (in boldface) of pcDNA3.1-Myc-His to generate pJSK37.

10^7 HEK293 cells were transfected with pJSK37 using the Polyfect transfection reagent (Qiagen). Cells were rinsed (twice) with ice-cold PBS, scraped off, and homogenized with a 26-gauge needle in 1 ml of buffer (25 mM Tris-HCl, pH 7.6, 1 mM EGTA, aprotinin (5 μg/ml), leupeptin (10 μg/ml), and 1 mM Pefabloc). His-tagged PE_PGRS33 was purified from the cytosolic fraction by chromatography on Ni^{+2}-NTA-agarose.

LPS Assay—LPS contamination of the purified protein was determined by *Limulus amoebocyte* lysate assay using the E-TOXATE kit from Sigma with a sensitivity limit of 0.1 endotoxin unit/ml.

Ectopic Expression of His_6-PE-PGRS33 in M. smegmatis—Briefly, the *His-PE-PGRS33* gene was cloned in a shuttle vector carrying the mycobacterial and *E. coli* origins of replication under the control of the *hsp60* promoter (28) to generate pJSK101. For ectopic expression of His-PE_PGRS33, pJSK101 was electroporated into *M. smegmatis* mc^2155. Expression of His-PE-PGRS33 was confirmed by Western blotting of the lysates from exponentially growing *M. smegmatis*/pJSK101 with anti-His antibody.

Challenge of RAW 264.7 with Bacteria—RAW 264.7 cells were infected with *M. smegmatis* harboring vector alone or pJSK101 expressing PE_PGRS33 at multiplicities of infection of 5, 10, and 20 for various periods of time. Cytochalasin D was used to prevent internalization of bacteria (29). Cells were treated with cytochalasin D (5 μM) for 1 h followed by washing three times with PBS before infection with *M. smegmatis.* To determine the survival of bacteria within macrophages, infected macrophages were washed with PBS and lysed with 0.05% SDS. The lysates were serially diluted and plated on Middle Brook 7H11 agar, and colony-forming units were determined.

Isolation of Monocyte-derived Macrophages (MDM)—MDM were isolated as described by Manor and Sarov (30). Briefly, human peripheral blood monocytes were prepared from heparinized blood of normal healthy volunteers (with informed consent), by density gradient centrifugation on Ficoll-Paque (Sigma). Cells from the interface were washed three times, suspended in RPMI 1640 containing HEPES buffer, and incubated in plastic dishes for 2–3 h at 37 °C in a CO_2 incubator. Adherent monocytes were removed from the plate by gentle scraping. Monocytes obtained were incubated for 7–10 days in RPMI with 10% FBS in a CO_2 incubator when 95% of monocytes were converted to MDM.

Cell Death—For the detection of histones by ELISA, cells were plated (6×10^4cells/well) on 96-well plates. After treatments, cell death was detected with the cell death detection ELISA Plus kit (Roche Applied Science) according to the manufacturer's protocol. For measurements of annexin-fluos binding, 100 μl of cells in annexin-fluos binding buffer (10 mM HEPES, pH 7.4, 140 mM NaCl, and 2.5 mM $CaCl_2$) were mixed with 2 μl of annexin-fluos. The mixture was incubated for 15 min at room temperature, washed with binding buffer, and analyzed by flow cytometry. To assess necrosis, propidium iodide (1 μg/ml) was added to the cell suspension just before analysis. Unless otherwise stated, cell death was analyzed 20 h after challenge with PE_PGRS33 (or PE_PGRS62 or PE_PGRS48).

Study of the Interaction of PE_PGRS33 with TLR2—Lysates from RAW 264.7 cells (10^7 cells/assay) were incubated with Ni^{2+}-NTA or PE_PGRS33-bound Ni^{2+}-NTA-agarose at 4 °C for 2 h with shaking. The beads were washed and boiled in 2× Laemmli buffer for 5 min, and proteins were separated by 7.5% SDS-PAGE, transferred onto a polyvinylidene difluoride membrane, and immunoblotted with anti-TLR2 antibody to detect His-PE_PGRS33-bound TLR2. In separate experiments, HEK293 cells transfected either with TLR2 or with TLR4 were incubated for 10 min with His-PE_PGRS33. Plates were washed with PBS and scraped out in PBS containing 1% bovine serum albumin (BSA). Pelleted cells were incubated with rabbit anti-His antibody (Cell Signaling Technology, Beverly, MA) for 1 h at 4 °C. Pellets were washed twice with PBS and 1% BSA and incubated with 2 μg/ml Alexa 488-conjugated anti-rabbit IgG in 250 μl of PBS and 1% BSA for 45 min on ice. Pellets were washed twice, resuspended in 1 ml of PBS, and subjected to fluorescence-activated cell sorter analysis. 10,000 cells were counted for each condition.

Treatment of RAW 264.7 Cells with PE_PGRS33 and Preparation of Cell Lysates—RAW 264.7 cells were cultured in 24-well tissue culture plates at 4×10^5 cells/well, treated with PE_PGRS33, and lysed with lysis buffer (20 mM Tris-HCl, pH 7.4, containing 1% (v/v) Nonidet P-40, 10% (v/v) glycerol, 137 mM NaCl, 20 mM NaF, 1 mM EDTA, 40 mM sodium β-glycerophosphate, 4 μg/ml each of leupeptin, pepstatin, and aprotinin, 1 mM Na_3VO_4, 1 mM Pefabloc, and 1 mM benzamidine) on ice for 15 min. Cell lysates were boiled for 5 min after the addition of 5× Laemmli sample buffer and subjected to Western blotting. When performing Western blotting for detection of caspases, cells were pelleted and freeze-thawed three times in 20 μl of cell extraction buffer (50 mM PIPES/NaOH, pH 6.5, containing 2 mM EDTA, 0.1% (w/v) CHAPS, 5 mM dithiothreitol, 20 μg/ml leupeptin, 10 μg/ml pepstatin, 10 μg/ml aprotinin, and 1 mM Pefabloc). The lysates were centrifuged at 10,000 × *g* for 5 min at 4 °C, and the supernatants were collected for the detection of caspases.

Western Blotting—Proteins were separated on SDS-polyacrylamide gels and then transferred electrophoretically to polyvinylidene difluoride membranes. The blots were blocked with 5% nonfat dry milk and subsequently incubated overnight at 4 °C with primary antibodies in Tris-buffered saline containing 1% (v/v) Tween 20 (TBST) and 5% (w/v) BSA. After washing, the blots were incubated with horseradish peroxidase-conjugated goat anti-rabbit IgG (Cell Signaling Technology) (or appropriate secondary antibody) in blocking buffer for 1 h at room temperature, followed by development with BM chemiluminescence reagent (Roche Applied Science), and exposed to x-ray film (Kodak XAR5; Eastman Kodak Co.).

ASK1 Kinase Assay—This was done as described by Bhattacharyya *et al.* (31). RAW 264.7 cells were cultured in 24-well tissue culture plates at 6×10^5 cells/well. After treatment, cells were lysed with lysis buffer containing 20 mM Tris-HCl, pH 7.5, 150 mM NaCl, 1 mM EDTA, 1 mM EGTA, 1% (v/v) Triton X-100, 1% sodium deoxycholate, 0.5 mM sodium pyrophosphate, 1 mM sodium β-glycerophosphate, 1 mM Na_3VO_4, and 1 μg/ml leupeptin. The supernatant (equivalent to 200 μg of protein) was incubated overnight at 4 °C with rabbit polyclonal ASK1 antibody. Protein A/G Plus-agarose was added and incubated at 4 °C for an additional 3 h. The beads were washed twice with lysis buffer and twice with kinase buffer (25 mM Tris-HCl, pH 7.5, containing 5 mM sodium β-glycerophosphate, 2 mM dithiothreitol, 0.1 mM Na_3VO_4, and 10 mM $MgCl_2$). The pellet was washed once with kinase buffer without protease inhibitors. The beads were then incubated in 20 μl of kinase buffer in the presence of 0.5 μCi of [γ-^{32}P]ATP (specific activity, 6000 Ci/mmol) with 1 μg of myelin basic protein as substrate at 30 °C for 15 min. The reaction was stopped by adding protein gel denaturing buffer. After SDS-PAGE, gels were dried and subjected to autoradiography.

Isolation of Cytosol and Mitochondrial Fractions for Detection of Cyt c and Bid—After the treatments, 18×10^6 cells were suspended in 400 μl of suspension buffer (20 mM HEPES, pH 7.5, containing 10 mM KCl, 1.5 mM $MgCl_2$, 1 mM EDTA, 1 mM EGTA, 1 mM Pefabloc, 10 μg/ml leupeptin, 10 μg/ml aprotinin, and 150 mM sucrose) and broken by 20 passages through a 26-gauge needle. The homogenate was centrifuged at 750 × *g* for 10 min to remove nuclei and unbroken cells. The mitochondrial pellet was obtained by centrifugation at 10,000 × *g* for 15 min and resuspended in 40 μl of resuspension buffer (20 mM

Tris-HCl, pH 7.4, containing 100 mM NaCl, 1 mM Pefabloc, 10 μg/ml leupeptin, and 10 μg/ml aprotinin). The supernatant obtained by centrifugation at 100,000 × *g* for 60 min at 4 °C was the cytosolic fraction. Before Western blotting, protein concentrations were assayed, and all samples were normalized to equal protein concentrations. Blots probed with anti-cyt *c* antibody were stripped and reprobed for β-actin expression to confirm equal loading in all lanes.

Measurement of Mitochondrial Membrane Potential—The induction of the mitochondrial permeability transition was determined in intact cells as the reduction in the accumulation of $DiOC_6$ (32). Briefly, 5×10^5 RAW 264.7 cells were loaded with $DiOC_6$ (100 nM) during the last 30 min of treatment with PE_PGRS33 and then lysed in deionized water, and fluorescence of $DiOC_6$ was read in a Hitachi F-4500 fluorescence spectrophotometer at excitation and emission wavelengths of 488 and 500 nm, respectively. Values for de-energized mitochondria were determined by simultaneous treatment of cells with 10 μM carbonyl cyanide *m*-chlorophenylhydrazone (CCCP) and $DiOC_6$.

Measurement of TNF-α in Culture Supernatants—Cells after treatment with inhibitors or after transfections were incubated with PE_PGRS33 (or its mutants) or PE_PGRS62 or PE_PGRS48. The conditioned medium was removed and assayed for TNF-α by ELISA using the murine Biotrak TNF-α assay kit (Amersham Biosciences) according to the manufacturer's protocol.

RNA Isolation and RT-PCR—Total RNA was prepared from cells using the RNeasy mini kit (Qiagen) according to the manufacturer's protocol. 100 ng of RNA was reverse-transcribed using the Titanium One-step RT-PCR kit (Clontech). The sense and antisense primers 5′-GGCAGGTCTACTTTGGAGTCATTGC-3′ and 5′-ACATTCGAGGCTCCAGTGAATTCGG-3′, respectively, were used to amplify 299 bp of the murine TNF-α mRNA. The sense and antisense primers 5′-CGGACATGGGTCTCCCCACCG-3′ and 5′-AACCCTGCATGGCAG-3′, respectively, were used to amplify 529 bp of the murine TNFRI mRNA. The PCR conditions for TNF-α mRNA amplification were denaturation at 94 °C for 30 s, annealing at 60 °C for 30 s, and extension at 68 °C for 1 min for 35 cycles. For TNFRI, annealing was carried out at 52 °C. Glyceraldehyde-3-phosphate dehydrogenase (*gapdh*) was amplified using the primers 5′-CCA TCA ATG ACC CCT TCA TTG ACC-3′ (sense) and 5′-GAA GGC CAT GCC AGT GAG CTT CC-3′ (antisense) to generate a 604-bp product.

Analysis of Surface Expression of TNFRI by Flow Cytometry—Surface-exposed TNFRI was quantitated by flow cytometry. Cells before or after treatment were incubated with TNFRI antibody or isotype control IgG for 30 min, washed with PBS, and incubated with Alexa-488-conjugated anti-rabbit IgG for 30 min. The cells were then washed three times with PBS and analyzed by flow cytometry. 10,000 cells were counted for each condition.

Statistical Analysis—Data are represented as the means ± S.D. of separate experiments. Analysis of variance and Student's *t* test were performed to test statistical significance. A *p* value of <0.05 was considered statistically significant.

RESULTS

PE_PGRS33 Stimulates Release of TNF-α from RAW 264.7 Macrophages—The ability of His-PE_PGRS33 to stimulate TNF-α release was studied in the macrophage cell line RAW 264.7. Recombinant His-PE_PGRS33 stimulated the release of TNF-α from RAW 264.7 macrophages in a time-dependent (Fig. 1*A*) and dose-dependent manner (Fig. 1*B*).

PE_PGRS33-induced TNF-α Release Is Neither Because of His Tag nor LPS—To control for nonspecific effects of the His tag present in recombinant PE_PGRS33, the TNF-α-inducing ability of two different His-tagged PE_PGRS proteins was tested in parallel. Neither His-tagged PE_PGRS48 nor PE_PGRS62 could induce TNF-α release above the level observed in control cells (Fig. 1*C*), ruling out the likelihood of the His tag contributing toward the TNF-α-inducing ability. These results also suggest that the TNF-α-inducing ability is specific for PE_PGRS33 and is not a common feature of the PE_PGRS family. Heat treatment inhibited the TNF-α-inducing ability of PE_PGRS33 (Fig. 1*C*), whereas polymyxin B treatment was without effect (Fig. 1*C*), ruling out the possibility that the observed induction of TNF-α was because of the contamination of LPS. The PE domain of PE_PGRS33 alone was not able to elicit the release of TNF-α (Fig. 1*D*). This further suggests that the observed effects are dependent on the PGRS domain of PE_PGRS33 rather than being attributable to any contaminating factors. His-PE_PGRS33 was also expressed and purified from HEK293 cells. This protein could also elicit TNF-α release from RAW 264.7 macrophages (Fig. 1*C*). This confirmed that the observed effect of PE_PGRS33 was not because of contaminating bacterial products.

Mutations of PE_PGRS33 Affect TNF-α Release—Taking the gene sequence of PE_PGRS33 of *M. tuberculosis* H37Rv as reference, Talarico *et al.* (26) have recently shown a large number of sequence variations in the *PE_PGRS33* gene in clinical isolates of *M. tuberculosis*. These variations include synonymous and nonsynonymous single nucleotide polymorphisms, in-frame insertions and deletions, and deletion resulting in frameshift, which were mainly found in the PGRS-encoding domain. To relate these genetic variations with the TNF-α-inducing ability of PE_PGRS33, we mimicked some of these mutations by genetic manipulation of *PE_PGRS33*, expressed the corresponding recombinant proteins with a His tag, and studied the release of TNF-α by these variants. Point mutations S178A, V234A, G320A, G389A, T391I, and deletions of amino acids Gly-217 to Gly-219, Gly-227 to Gly-229, and Ala-198 to Gly-203, all variations in the PGRS domain, did not have significant effect on TNF-α-inducing ability of exogenous PE_PGRS33. However, the deletions from Gly-184 to Gly-213, from Gly-196 to Asp-243, from Leu-237 to Gly-327, and from Gly-372 to Ala-403 all attenuated PE_PGRS33-induced release of TNF-α from RAW 264.7 cells (Fig. 1*D*).

PE_PGRS33 Signals through TLR2—To test whether PE_PGRS33 signals by interacting with cell surface receptors, we focused on the TLR family. Transfection of RAW 264.7 with dominant-negative TLR2, but not with dominant-negative TLR4, inhibited the TNF-α-inducing ability of PE_PGRS33 (Fig. 2*A*) suggesting that PE_PGRS33 likely signals through

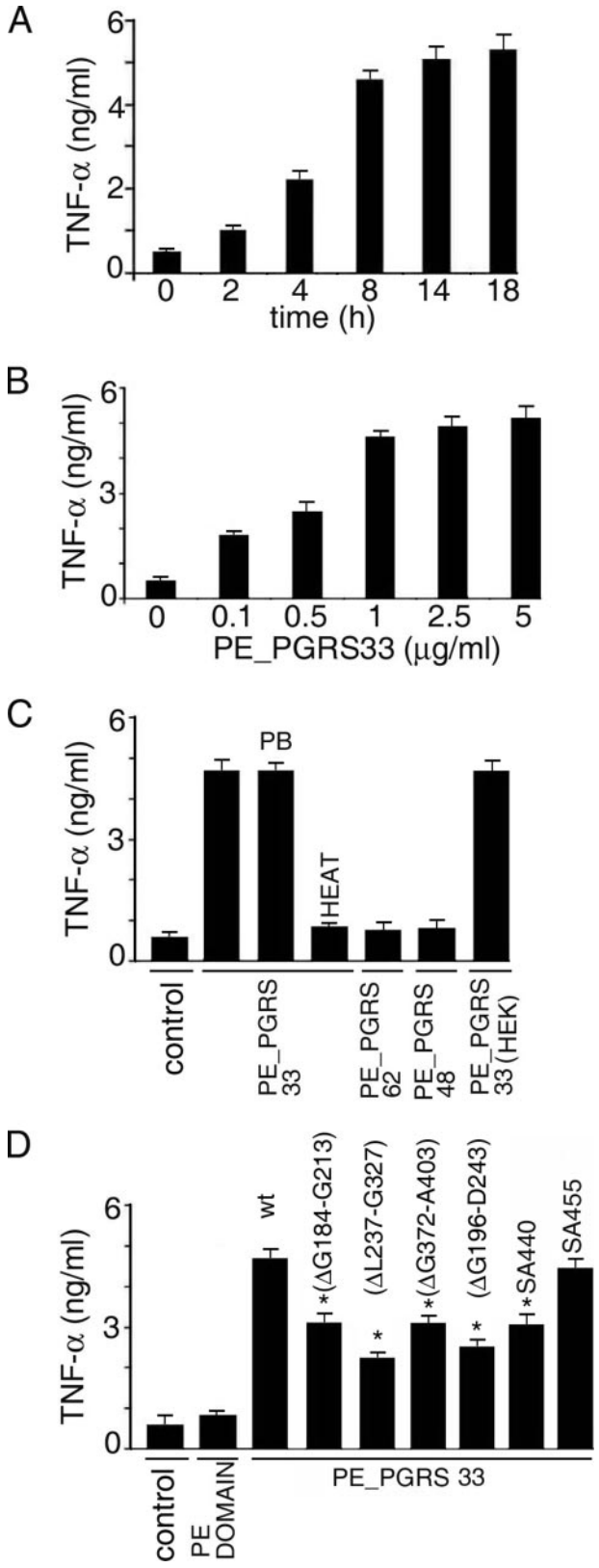

FIGURE 1. **Release of TNF-α induced by PE_PGRS33.** RAW 264.7 cells were incubated with PE_PGRS33 (1 μg/ml) for different periods of time (*A*) or with different concentrations of PE_PGRS33 for 14 h (*B*). *C,* PE_PGRS33 was subjected to boiling for 1 h (heat) or was treated with polymyxin B (*PB*) resin. For the latter, 100 μl of PE_PGRS33 was mixed with 100 μl of polymyxin B resin and incubated at 4 °C for 1 h. Beads were removed, and the supernatant was used to induce TNF-α. In all experiments recombinant PE_PGRS33 purified from *E. coli* was used unless otherwise stated. In separate experiments, cells were treated with recombinant PE_PGRS33 or PE_PGRS62, or PE_PGRS48 (produced in *E. coli*) as indicated. Cells were also treated with recombinant PE_PGRS33 produced in HEK293 (PE_PGRS33 (HEK)) at a concentration of 1 μg/ml. *D,* cells were treated with recombinant full-length PE_PGRS33 (*wt*) or the PE domain (amino acid residues 1–140) or different mutants of PE_PGRS33 as indicated. SA440 represents PE_PGRS33 expressed from a gene carrying a 107-bp deletion from 710 to 816 bp (36 amino acids), as well a 32-bp insertion at 817 bp (after amino acid 272, leading to the insertion of 11 amino acids). SA455 represents PE_PGRS33 expressed from a gene carrying a single nucleotide polymorphism (T → C transition at position 717), a 9-bp insertion at 1240 bp (resulting in the insertion of a Gly-Ala-Gly sequence after amino acid 413) and an 18-bp insertion at 597 bp (resulting in the insertion of Gly-Ala-Gly-Gly-Ala-Gly after amino acid 199). The numbering is based on the nucleotide and amino acid sequences of PE_PGRS33 of *M. tuberculosis* H37Rv. In all cases incubation was carried out for 14 h, and released TNF-α was measured in the supernatant. All values are means ± S.D. for three separate sets of experiments. *, $p < 0.01$; *versus* control treated with full-length PE_PGRS33 of *M. tuberculosis* H37Rv (WT).

TLR2. The HEK293 cell line does not express TLR2 or TLR4. To confirm our view that PE_PGRS33 signals specifically through TLR2, we transfected HEK293 cells either with TLR2 or with TLR4. PE_PGRS33 could elicit TNF-α release from HEK293 cells transfected with TLR2 but not from HEK293 cells transfected with TLR4 (Fig. 2*B*). PE_PGRS33 could also elicit TNF-α release from MDM (Fig. 2*C*). This could be blocked by neutralizing antibody against TLR2 (Fig. 2*C*) but not with neutralizing antibody against TLR4 (Fig. 2*C*) or isotype-specific antibody (data not shown) further supporting a crucial role of TLR2 in PE_PGRS33-mediated TNF-α release.

Interaction of PE_PGRS33 with TLR2—To test whether PE_PGRS33 interacts with TLR2, RAW 264.7 cell lysates were incubated with PE_PGRS33 immobilized on Ni^{2+}-NTA-agarose. Western blots probed with anti-TLR2 antibody showed that TLR2 was pulled down with immobilized PE_PGRS33 in the absence or in the presence of polymyxin B (Fig. 2*D*), suggesting an interaction between PE_PGRS33 and TLR2 independent of any possible contamination by LPS. TLR2 could not be pulled down either in a control tube containing Ni^{2+}-NTA-agarose alone or when an irrelevant His-tagged protein was immobilized on Ni^{2+}-NTA agarose, confirming a specific interaction between PE_PGRS33 and TLR2. No band appeared in Western blots performed using anti-CD14 or anti-TLR4 antibody as negative controls (data not shown), confirming that the band that was visible after pulldown could be attributed specifically to TLR2. To confirm that TLR2 was the receptor of PE_PGRS33, we also analyzed the binding of PE_PGRS33 to TLR2-transfected HEK293 cells by flow cytometry. There was a dose-dependent increase in PE_PGRS33 binding to TLR2-transfected HEK293 cells (Table 2). We also tested binding of PE_PGRS33 to HEK293 cells transfected with TLR4. In this case, binding of Alexa-488 did not show any increase in concentrations of PE_PGRS33 (up to a concentration of 5 μg/ml) (data not shown). These results argued in favor of a specific interaction between PE_PGRS33 and TLR2.

TNF-α Release from Macrophages Challenged with M. smegmatis Harboring PE_PGRS33—To analyze the effects of PE_PGRS33 on RAW 264.7 macrophages in the context of the bacterium as a whole, we compared the relative ability of transformants of *M. smegmatis* ectopically expressing PE_PGRS33 or harboring the empty vector alone to release TNF-α. PE_PGRS33 expressed in *M. smegmatis* has been demonstrated to

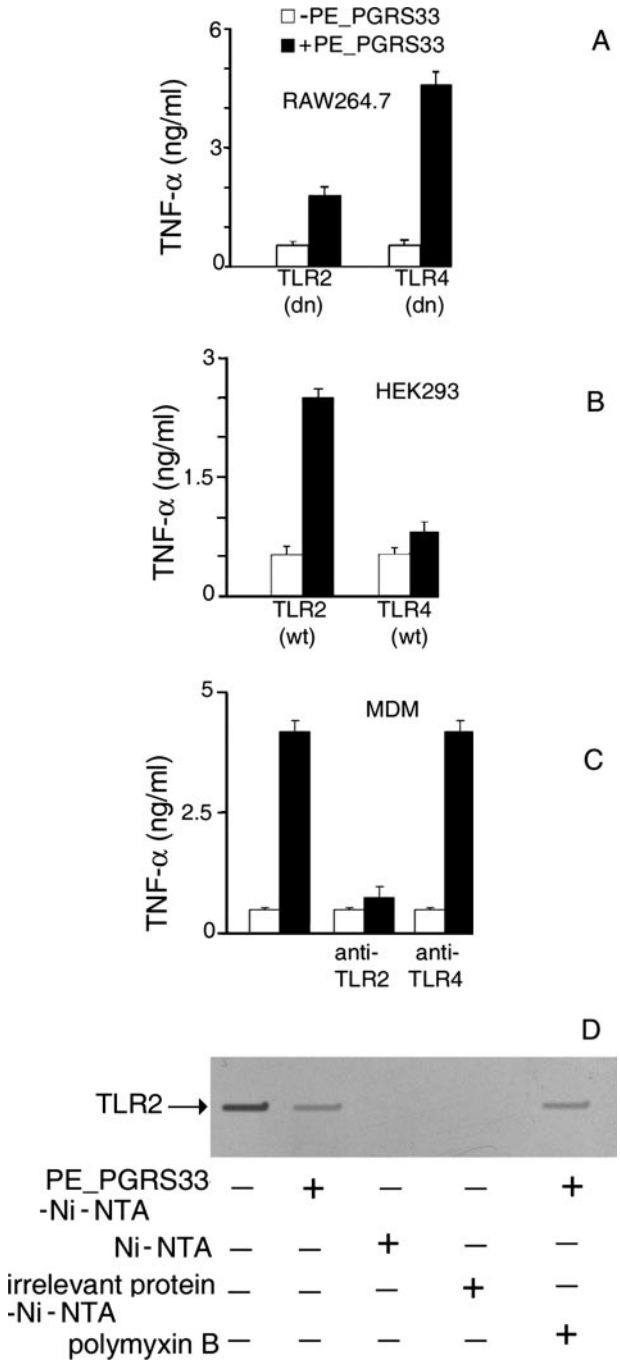

FIGURE 2. **PE_PGRS33 signals through TLR2.** RAW 264.7 (*A*) or HEK293 (*B*) cells were transfected with wild type (*wt*) or dominant-negative (*dn*) TLR constructs as indicated. Transfected cells were either left untreated (□) or treated (■) with PE_PGRS33 (1 μg/ml) for 14 h. *C*, human peripheral blood MDM were pretreated with neutralizing anti-TLR2 or -TLR4 antibody for 1 h. Cells were then incubated without or with PE_PGRS33 (1 μg/ml) in fresh medium for 14 h. In all cases, the release of TNF-α was measured in the supernatant. Values are the means ± S.D. of three different experiments. *D*, lysate from RAW 264.7 cells was incubated with PE_PGRS33 immobilized with Ni^{2+}-NTA-agarose in the absence or presence of polymyxin B or with Ni^{2+}-NTA-agarose alone or with an irrelevant His-tagged protein immobilized on Ni^{2+}-NTA-agarose for 2 h; the agarose-bound proteins were separated by SDS-PAGE and immunoblotted with anti-TLR2 antibody. The *1st lane* is the positive control representing immunoprecipitated TLR2 only.

be surface-expressed (20). RAW 264.7 cells were challenged with *M. smegmatis* containing the vector alone or the vector harboring the *PE_PGRS33* gene at a multiplicity of infection of

TABLE 2
Binding of PE_PGRS33 to TLR2-transfected HEK293

His-PE_PGRS33	% Alexa-488-positive cells[a]
μg/ml	
0	8 ± 1
0.5	32 ± 4[b]
1.0	58 ± 5[b]
2.0	60 ± 6[b]

[a] The results represent the means ± S.D. of three separate determinations.
[b] $p < 0.001$ *versus* cells not exposed to His-PE_PGRS33.

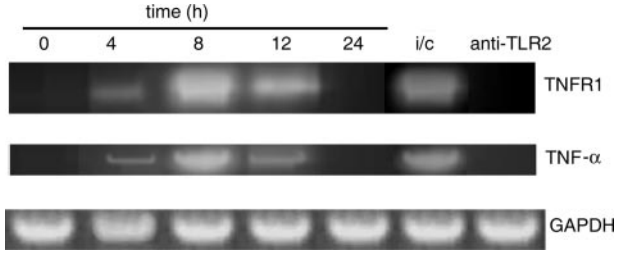

FIGURE 3. **RT-PCR analysis of PE_PGRS33-induced expression of *TNFRI* and *TNF-α*.** RAW 264.7 cells were left untreated or treated with PE_PGRS33 for different periods of time. In a separate experiment, cells were pretreated with neutralizing TLR2 antibody (*anti-TLR2*) or isotype IgG (*i/c*) for 1 h, followed by incubation with PE_PGRS33 for 8 h. RNA was isolated from the cells, and RT-PCR was carried out according to the manufacturer's protocol. DNA was separated on agarose gel and visualized by staining with ethidium bromide. Glyceraldehyde-3-phosphate dehydrogenase (*GAPDH*) was amplified as control for all experiments.

10 for various periods of time. Macrophages infected with *M. smegmatis* release TNF-α (8). This likely depends both on signals originating at the cell surface and on signals generated by intracellular PRRs. Based on our observations that PE_PGRS33 interacts with TLR2, we confined our interest to analyzing specifically the effect of interaction of PE_PGRS33 with surface-exposed receptors. Internalization of the bacteria was inhibited by preexposure to cytochalasin D, an actin depolymerization drug (to inhibit phagocytosis). Inhibition of phagocytosis was confirmed by determining colony-forming units before and after challenge of cytochalasin D-treated RAW 264.7 cells with *M. smegmatis*. For TNF-α measurement, *M. smegmatis* was added to cytochalasin D-treated RAW 264.7. 18 h after challenge, *M. smegmatis* harboring empty vector released 1 ± 0.2 ng/ml ($n = 4$) TNF-α from RAW 264.7 macrophages, whereas *M. smegmatis* harboring the *PE_PGRS33* gene released 4 ± 0.5 ng/ml TNF-α from RAW 264.7 ($n = 4$). TNF-α release decreased to the level of 1 ± 0.3 ng/ml ($n = 4$) when cytochalasin D-treated cells were also pretreated with neutralizing anti-TLR2 antibody, suggesting that the initial interaction of PE_PGRS33 with surface-exposed TLR2 was sufficient for TNF-α release. The above results suggest that PE_PGRS33 expressed in the bacterium gives the bacterium the ability to elicit TNF-α in a TLR2-dependent manner.

PE_PGRS33 Stimulates TNF-α Gene Expression—To determine whether the effect of PE_PGRS33 on TNF-α release was attributable to regulation at the level of *TNF-α* gene transcription, we analyzed the expression of *TNF-α* in PE_PGRS33-challenged macrophages by RT-PCR. Compared with untreated cells, PE_PGRS33 elicited the time-dependent expression of *TNF-α* (Fig. 3). This was abrogated in cells pretreated with neutralizing antibody against TLR2 (Fig. 3), suggesting that the

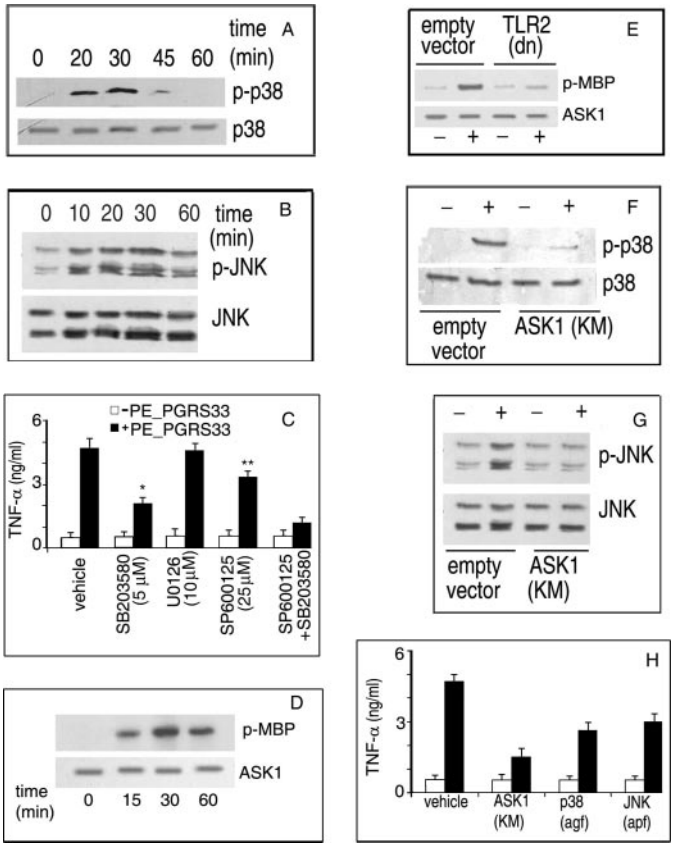

FIGURE 4. **PE_PGRS33-induced TNF-α release depends on ASK1 and MAPKs.** *A* and *B,* RAW 264.7 cells were left untreated or treated with PE_PGRS33 (1 μg/ml) for different periods of time. Cell lysates were prepared and separated on SDS-PAGE followed by immunoblotting with antibody against phospho-p38 or phospho-JNK MAPK. *C,* RAW 264.7 cells were treated with vehicle alone or MAPK inhibitors individually or in combination for 60 min followed by removal of inhibitors and incubation without (□) or with (■) PE_PGRS33 (1 μg/ml) for 14 h. The release of TNF-α was measured in the supernatant. *, $p < 0.001$; **, $p < 0.05$, *versus* control (vehicle) treated with PE_PGRS33. *D* and *E,* RAW 264.7 cells were treated with PE_PGRS33 for different periods of time (*D*), or cells were transfected with empty vector or dominant-negative (*dn*) TLR2 (*E*) followed by treatment without (−) or with (+) PE_PGRS33. Cell lysates were prepared, ASK1 was immunoprecipitated, and *in vitro* ASK1 kinase activity was determined using myelin basic protein (*MBP*) as substrate as described under "Experimental Procedures." *F* and *G,* cells were transfected with empty vector or kinase-dead ASK1 (ASK1(KM)) as indicated, followed by treatment without or with PE_PGRS33 as stated under *E.* Phospho-p38 (*F*) or phospho-JNK (*G*) was analyzed by Western blotting as described under *A* and *B. H,* cells were transfected with empty vectors or dominant-negative constructs indicated, followed by incubation without (□) or with (■) PE_PGRS33 (1 μg/ml) for 14 h. The release of TNF-α was measured in the supernatant. Blots shown are representative of the results obtained in three separate sets of experiments. Lower blots of *A, B, F,* and *G* were probed with nonphospho-antibodies to confirm equal loading in all lanes. For *D* and *E,* Western analysis with anti-ASK1 antibody (*lower panels*) was performed to confirm equal loading in all lanes. For *C* and *H*, values are means ± S.D. for three separate sets of experiments.

TLR2-dependent regulation of TNF-α release by PE_PGRS33 is likely at the transcriptional level.

PE_PGRS33-induced TNF-α Release Is Dependent on the MAPKs p38 and JNK—To elucidate the PE_PGRS33-induced signaling downstream of TLR2, we focused on the MAPKs. PE_PGRS33 elicited a time-dependent activation of p38 (Fig. 4*A*) and JNK (Fig. 4*B*) MAPKs. It was observed that inhibition of ERK1/2 signaling by U0126 did not affect TNF-α release (Fig. 4*C*). On the other hand, treatment of cells with the p38 MAPK inhibitor SB203580 or the JNK inhibitor SP600125 led to decrease in TNF-α release (Fig. 4*C*) A combination of both inhibitors could inhibit the release of TNF-α to the extent of >90%. Taken together, these results suggest that PE_PGRS33-mediated TNF-α release is dependent on signaling mediated by the MAPKs p38 and JNK.

PE_PGRS33-induced TNF-α Release Depends on the TLR2-dependent Activation of the Mitogen-activated Protein Kinase Kinase Kinase (MAPKKK) ASK1—The activation of the stress-activated protein kinases p38 and JNK is the culmination of a cascade of phosphorylation events mediated by MAPKK and MAPKKK. The MAPKKK ASK1 is a key mediator in p38 and JNK activation (33–35). The role of ASK1 in mycobacteria-mediated signaling in macrophages has been demonstrated by us in previous studies (31). ASK1 has also been shown to induce p38 MAPK activation downstream of TLR2 signaling initiated by mycoplasmal lipoprotein and staphylococcal peptidoglycan (36). In the present instance, PE_PGRS33 was found to activate ASK1 in a time-dependent manner (Fig. 4*D*). Transfection of RAW 264.7 cells with dominant-negative TLR2 abrogated the activation of ASK1, suggesting that PE_PGRS33-mediated ASK1 activation is dependent on TLR2 (Fig. 4*E*). At the same time, ASK1(KM) could inhibit the activation of p38 (Fig. 4*F*) and JNK (Fig. 4*G*) MAPKs as well as the release of TNF-α (Fig. 4*H*). Taken together, these results support the view that the TLR2/ASK1/p38, JNK signaling axis is central to the PE_PGRS33-induced release of TNF-α.

PE_PGRS33-mediated Cell Death Is Dependent on TNF-α—Considering that activation of ASK1 and TNF-α have in many instances been related to the triggering of apoptotic signaling, we investigated whether PE_PGRS33 could induce cell death in RAW 264.7 cells. PE_PGRS33 could induce apoptosis in RAW 264.7 cells in a time- (Fig. 5*A*) and dose-dependent manner (Fig. 5*B*) as assessed by histone ELISA. Cell death was also assessed by measuring the binding of annexin-fluos to treated cells. This method also supports the view that PE_PGRS33 is an apoptosis-inducing protein (Table 3). Using propidium iodide staining, no necrosis was observed in the treated cells. Other PE_PGRS proteins such as PE_PGRS62 and PE_PGRS48 were unable to induce cell death in RAW 264.7 macrophages, suggesting that the death-inducing property is not common to all members of this family.

We next evaluated whether PE_PGRS33 expressed by *M. smegmatis* could elicit macrophage cell death. To exclude effects exerted by *M. smegmatis* only after internalization, RAW 264.7 cells were pretreated with cytochalasin D as described above. Cells were then challenged with *M. smegmatis* harboring vector alone. 24 h after challenge, no significant increase in histone release over that in cells that had not been challenged with the bacteria was observed. *M. smegmatis* harboring the *PE_PGRS33* gene could, on the other hand, elicit a 4 ± 0.5-fold ($n = 4$, $p < 0.05$) greater release of histone in cytochalasin D-treated RAW 264.7 compared with cells that had not been challenged with the bacteria. Pretreatment of cells with anti-TLR2-neutralizing antibody abrogated the ability of *M. smegmatis*/PE_PGRS33 to elicit cell death in cytochalasin D-treated RAW 264.7 cells (data not shown).

TLR2 can recruit Fas-associated death domain to stimulate apoptosis in a variety of situations (37). Because PE_PGRS33

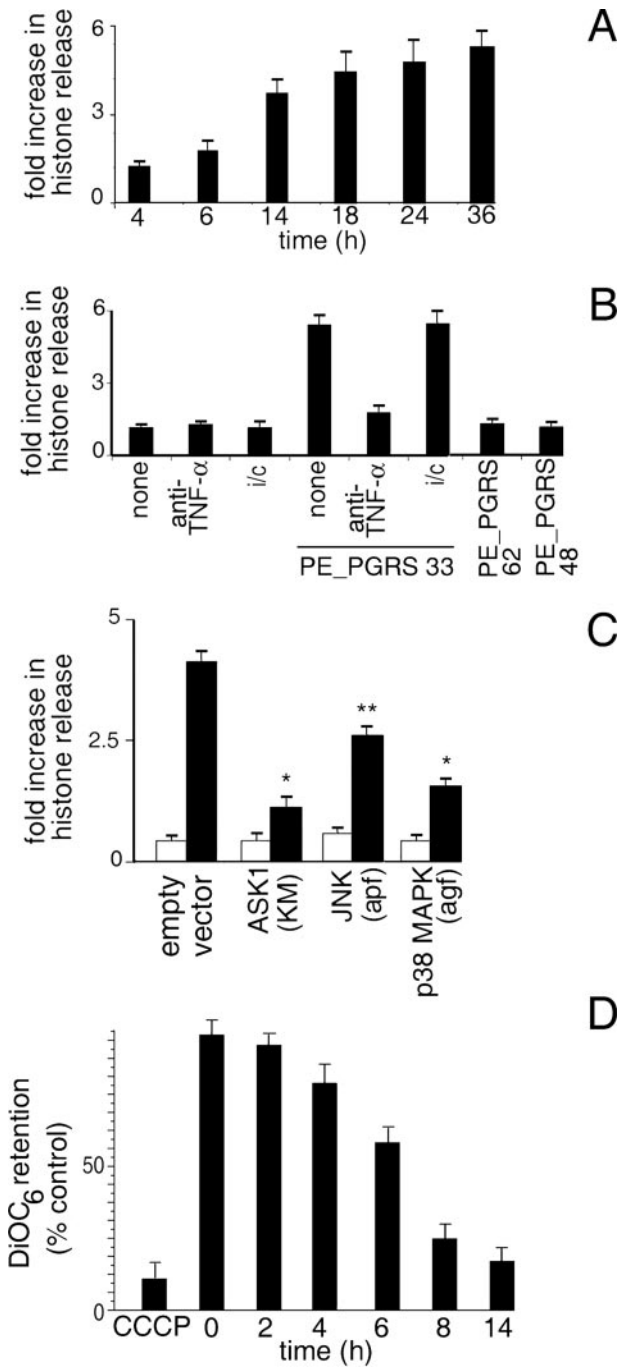

FIGURE 5. **PE_PGRS33-induced loss of mitochondrial membrane potential and cell death.** RAW 264.7 cells were either left untreated or treated with PE_PGRS33 (1 μg/ml) for different periods of time (*A*). In a separate experiment, cells were either left untreated or pretreated with TNF-α neutralizing antibody (10 μg/ml) or with isotype IgG (*i/c*) for 1 h (*B*) followed by incubation with PE_PGRS33. In separate experiments, cells were also treated either with PE_PGRS62 or PE_PGRS48. *C*, cells were transfected with empty vector or dominant-negative constructs as indicated. Cells after transfection were either left untreated (□) or treated with PE_PGRS33 (■). In each case, the inducer was removed, and cells were washed and lysed, and cell death was measured using the cell death ELISA kit from Roche Applied Science as described under "Experimental Procedures." Results are expressed as fold increase in the release of histone in comparison with that of the control (untreated RAW 264.7). *, $p < 0.001$; **, $p < 0.01$, *versus* control. *D*, cells were treated with PE_PGRS33 for different periods of time. Cells were washed, and the fluorescence of $DiOC_6$ was determined at excitation and emission wavelengths of 488 and 500 nm, respectively. Values for deenergized mitochondria were determined by simultaneous treatment of cells with 10 μM CCCP and $DiOC_6$. Values are given as means ± S.D. of three different experiments.

TABLE 3
PE_PGRS33- induced apoptosis in RAW 264.7 cells

	Annexin V-fluos-positive cells (%)[a]
Control	8 ± 1
His-PE_PGRS33	70 ± 8[b]
His-PE_PGRS33 + anti-TNF-α[c]	10 ± 1[d]
His-PE_PGRS33 + i/c[c]	72 ± 6[b]
His-PE_PGRS33 + z-IETD-FMK	15 ± 3[d]
His-PE_PGRS33 + z-LEHD-FMK	16 ± 3[d]
His-PE_PGRS33 + z-DEVD-FMK	13 ± 2[d]
His-PE_PGRS33 + PB[e]	70 ± 6[b]
Heat-treated His-PE_PGRS33	7 ± 1[d]
Irrelevant His-protein	8 ± 1[d]
His-PE_PGRS (HEK) expressed in, and purified from HEK 293	73 ± 8[b]

[a] Results represent the means ± S.D. of three separate determinations. His-PE_PGRS33 and His-PE_PGRS (HEK) represent the proteins expressed in *E. coli* and HEK293, respectively.
[b] Values are $p < 0.001$ *versus* control.
[c] Cells were pretreated with anti-TNF-α or isotype-matched antibody before treatment with PE_PGRS33.
[d] Values are $p < 0.001$ *versus* His-PE_PGRS33.
[e] PE_PGRS33 was incubated with polymyxin B resin before incubation with RAW 264.7.

signals through TLR2, we asked the question whether PE_PGRS33 was eliciting TLR2-dependent cell death independent of TNF-α release or whether the release of TNF-α was necessary for cell death. Pretreatment of RAW 264.7 with neutralizing antibody against TNF-α abrogated PE_PGRS33-induced cell death (Fig. 5*B*). This suggests that the release of TNF-α is essential for PE_PGRS33-dependent cell death. TNF-α triggers death receptor-dependent apoptosis by engaging TNFRI. PE_PGRS33 was capable of up-regulating expression of the *TNFRI* gene in a TLR2-dependent manner (Fig. 3). This was associated with increased cell surface expression of TNFRI. Surface expression of TNFRI was assessed by flow cytometry. Cells after exposure to PE_PGRS33 were treated with rabbit anti-TNFRI antibody followed by Alexa 488-conjugated secondary antibody. The binding of Alexa-488 served as a measure of surface exposure of TNFRI. There was a 3-fold increase in the surface expression of TNFRI in PE_PGRS33 -treated cells compared with untreated cells. The percent of Alexa-488-positive cells increased from 23 ± 4 (untreated cells) to 73 ± 4 ($n = 5$, $p < 0.001$) in PE_PGRS33-treated cells. Control experiments were performed using isotype IgG instead of TNFRI antibody, and no increase in Alexa 488 staining was observed in the absence or presence of PE_PGRS33.

PE_PGRS33-induced Cell Death Depends on ASK1/MAPK Signaling and Activation of Caspases—Transfection of cells with ASK1(KM), p38 (agf), and JNK (apf), inhibited PE_PGRS33-dependent cell death (Fig. 5*C*), suggesting a role of the ASK1/MAPK signaling axis in the cell death process. At the same time, pretreating cells with the caspase 3, 8, and 9 inhibitors Z-DEVD-FMK, Z-IETD-FMK, and Z-LEHD-FMK, respectively, led to an inhibition of PE_PGRS33-induced cell death as assessed by measuring the binding of annexin-fluos (Table 3), suggesting the likely involvement of all three caspases in the death process.

PE_PGRS33-induced Cell Death in Macrophages Occurs in a Mitochondria-dependent Manner—The activation of caspase 9 in the intrinsic pathway of cell death is preceded by the mitochondrial permeability transition and loss of the mitochondrial

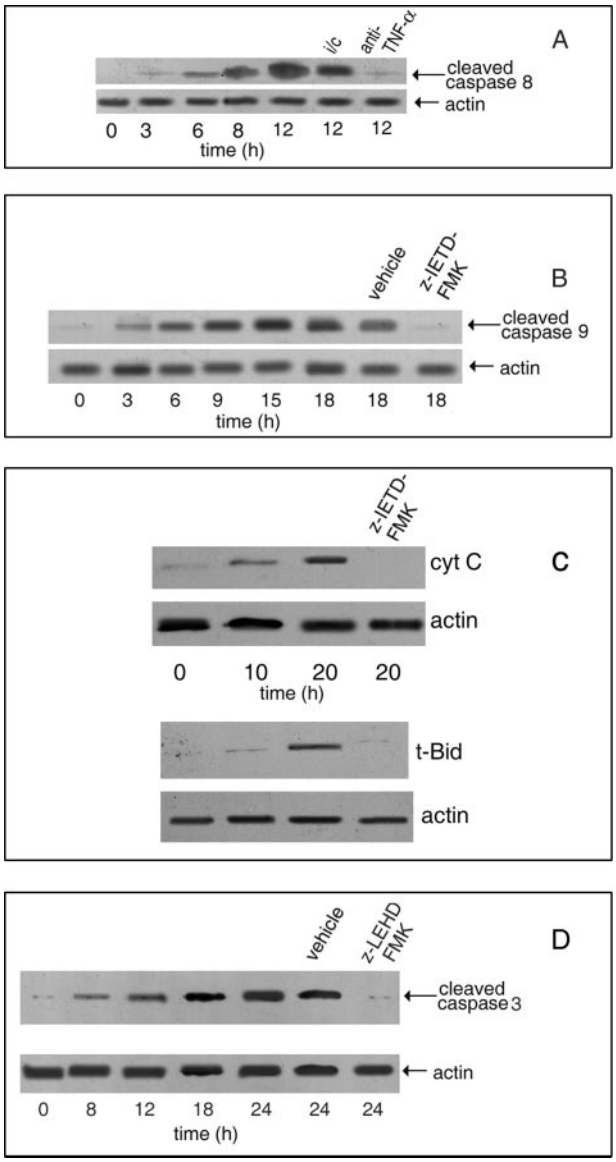

FIGURE 6. **PE_PGRS33-induced caspase activation and cleavage of Bid.** RAW 264.7 cells were either left untreated or treated with PE_PGRS33 (1 μg/ml) for different periods of time. Cell lysates were prepared as described under "Experimental Procedures." In a separate set of experiments, cells were pretreated with TNF-α neutralizing antibody or with isotype IgG (*i/c*) (*A*) as described under Fig. 4, with caspase 8 inhibitor (Z-IETD-FMK, 50 μM) (*B* and *C*), or with caspase 9 inhibitor (Z-LEHD-FMK, 50 μM) (*D*) for 1 h. Cleaved caspase 8 (20 kDa) (*A*) or caspase 9 (37 kDa, *B*), cyt *c* (*C*), t-Bid (*C*), and caspase 3 (17 kDa) (*D*) were detected by Western blotting using specific antibodies. Blots shown are representative of the results obtained in three separate sets of experiments.

membrane potential ($\Delta\psi_m$) (38). The mitochondrial permeability transition reduces the accumulation of the fluorescent dye $DiOC_6$ in the mitochondria as a consequence of the loss of $\Delta\psi_m$. We observed the activation of caspase 9 as assayed by Western blotting to detect the cleaved form of caspase 9 (Fig. 6*B*). As a positive control for monitoring loss of $\Delta\psi_m$, RAW 264.7 cells were treated with CCCP, a proton ionophore that dissipates $\Delta\psi_m$. A loss of $DiOC_6$ fluorescence was observed (Fig. 5*D*). A similar loss of $\Delta\psi_m$ was evident from the time-dependent reduction in accumulation of $DiOC_6$ (Fig. 5*D*) in PE_PGRS-challenged RAW 264.7 cells suggesting that the intrinsic pathway is involved in PE_PGRS33-mediated cell death.

Caspase 8 Activation Links the Mitochondrial Pathway to Death Receptor Signals in PE_PGRS33-mediated Cell Death—The PE_PGRS33-mediated activation of caspase 9 was inhibited by caspase 8 inhibitor Z-IETD-FMK (Fig. 6*B*), suggesting that death receptor-dependent apoptotic signals were likely amplified in a classical manner through caspase 8-triggered mitochondrial loss of $\Delta\psi_m$. Hallmarks of this pathway are the generation of truncated Bid (t-Bid), a proapoptotic member of the Bcl-2 family and the release of cytochrome *c* (39, 40). We could demonstrate the activation of caspase 8 (Fig. 6*A*), the generation of t-Bid (Fig. 6*C*), and the release of cytochrome *c* (Fig. 6*C*) arguing in favor of PE_PGRS33 triggering a classical death receptor-dependent signal undergoing amplification through the mitochondrial pathway by caspase 8-dependent insertion of t-Bid in the mitochondrial membrane.

Role of Caspase 3 in PE_PGRS33-mediated Cell Death—Consistent with the effect of caspase inhibitors on PE_PGRS33-induced cell death, Western analysis using antibodies specific for the cleaved form of caspase 3 showed that PE_PGRS33 challenge activated the executioner caspase 3 (Fig. 6*D*). The generation of cleaved caspase 3 could be blocked by pretreatment with the caspase 9-specific inhibitor Z-LEHD-FMK. Taken together, these results suggest that sequential activation of caspases 8, 9, and 3 downstream of TNF-α-dependent signaling is involved in PE_PGRS33-mediated cell death.

DISCUSSION

TNF- or TNFRs-deficient mice are compromised in their ability to combat pathogens such as *Listeria monocytogenes*, *M. tuberculosis*, *M. avium*, and *Salmonella typhimurium*. As hypothesized by Rahman and McFadden in a recent review (41), TNF signaling networks therefore provide a selection pressure for pathogens to evolve strategies to combat the TNF-mediated responses to infection. The PE_PGRS genes are restricted to mycobacteria, raising the interest in their role in the biology of *M. tuberculosis*. Clinical isolates undergo sequence variation of the PE_PGRS genes (26, 42), and extensive polymorphisms of members of this family have been shown in epidemiological studies (43). Comparison of the genome sequences of *M. tuberculosis* H37Rv and CDC1551 has revealed that 39 of 62 PE_PGRS genes show extensive sequence divergence that would result in the absence of a protein or a difference in size because of frame insertion or deletion or frameshift (42). We have tested the hypothesis that polymorphisms in at least one member of the PE_PGRS family, namely PE_PGRS33, could give rise to differences in the immune response that they elicit, focusing in this case on TNF-α. We have concentrated our efforts on PE_PGRS33, considering that it is surface-exposed, expressed during infection (18), and shows variations in its sequence among clinical strains (26).

The earliest phase of infection involves the interaction of the surface-exposed moieties of *M. tuberculosis* with the PRRs of macrophages. The outcome of these interactions dictates the course of the infection. Considering that PE_PGRS33 is surface-exposed, we felt that its effects on the early phases of the infection could be simulated by challenging macrophages with exogenous recombinant protein. The repertoire of immune response modulators released by *M. tuberculosis*-challenged

macrophages is central to the innate immune response. Following exposure of macrophages to recombinant PE_PGRS33, we evaluated the release of a number of cytokines/chemokines. PE_PGRS33 elicited the release of TNF-α in a TLR2-dependent manner. However, PE_PGRS33 did not induce the release of macrophage inflammatory protein-1α and -1β, monocyte chemoattractant protein-1, interleukin (IL)-6, IL-8, and IL-12 from RAW 264.7 (data not shown).

The role of TLR2 in PE_PGRS33-triggered TNF-α release was corroborated by challenging HEK293 cells expressing TLR2 with PE_PGRS33. Considering that PE_PGRS33 expressed and purified from HEK293 and from *E. coli* exerted similar effects, the possibility of bacterial contaminants playing a role in the process could be ruled out. Binding of PE_PGRS33 to TLR2-transfected HEK293 cells could be demonstrated by flow cytometry (Table 2). We extended our studies to evaluate whether point mutations, deletions, and insertions (classified based on the gene sequence of *M. tuberculosis* H37Rv as reference) in PE_PGRS33, reported in clinical strains (26), impacted the TLR2-dependent signaling elicited by PE_PGRS33. Although none of the point mutations had any effect, deletions ranging from 30 to 91 amino acids in the PGRS domain attenuated TNF-α release between 25 and 40%. The variant protein carrying two insertions of Gly-Ala-Gly repeats at two different positions did not show significant variation in TNF-α-releasing ability compared with PE_PGRS33 from *M. tuberculosis* H37Rv. It appears likely that the deletions analyzed caused structural alterations sufficient to affect the TLR2-binding capacity of the variant proteins. However, detailed analysis of the PE_PGRS33-TLR2 interaction interface will be required before definitive conclusions can be drawn. The expression of these variant proteins in clinical strains needs to be evaluated. In some instances, these deletions are reportedly associated with additional mutations (including insertions of Gly-Ala repeats). Assuming that the variant PE_PGRS proteins are expressed by clinical strains, our observations suggest that variations in the PGRS domain of PE_PGRS33 alter the levels of TNF-α induction and are therefore likely to have an impact on the innate immune response and on the course of infection.

Our observation that *M. smegmatis* harboring PE_PGRS33 could elicit TNF-α release from cytochalasin D-treated RAW 264.7 and that this could be inhibited by neutralizing antibody against TLR2 supports the view that interaction of PE_PGRS33 with surface-exposed TLR2 triggers a signaling pathway that constitutes at least one arm of signaling leading to TNF-α release, and that this pathway is of relevance in the context of the intact bacterium challenging the macrophage. Also of interest to the basic aspect of innate immunity was our observation that TNF-α release required the TLR 2/ASK1/p38-JNK signaling axis, showing that ASK1 activation downstream of TLR 2 has a role in the innate immune response to *M. tuberculosis* infection. This view is further supported by the recent report by Yang *et al.* (44) showing that TLR2/ASK1 signaling contributes to mycobacteria-induced IL-23 expression in macrophages.

TNF-α is a cytokine that is now acknowledged to be central to the outcome of tuberculosis. It plays a vital role by walling off the granuloma and containing the infection. In the present study, we explored whether it is part of an autocrine loop dictating the fate of the macrophage. Apoptosis of macrophages triggered by intracellular pathogens has been the subject of intense investigation in recent times. The interplay between pro-apoptotic and anti-apoptotic pathways in macrophages challenged with pathogenic mycobacteria, although incompletely understood to date, is nevertheless likely to have an important bearing on the outcome of the infection. The role of macrophage apoptosis in the context of *M. tuberculosis* infection is a complex one. Considering that the macrophage is its intracellular niche, virulent mycobacteria would be envisaged to thwart apoptosis in the early stages of infection. Indeed, virulent species of *M. tuberculosis* have been reported to evade apoptosis. Apoptosis of macrophages also contributes to the alternate pathway of T cell activation (14) giving reason to believe that *M. tuberculosis* would benefit from thwarting apoptosis. With the increase in bacterial load, however, the need for dissemination of the pathogen would lead to the pathogen benefiting from apoptotic and/or necrotic death of macrophages. PE_PGRS33 triggered apoptosis in macrophages. TLR2 may trigger apoptosis by direct recruitment of death effector domain-containing adapter proteins such as Fas-associated death domain (38). However, in the present instance, apoptosis was dependent on TLR2-dependent TNF-α release. The fact that PE_PGRS33 also triggered increased TNFRI expression, suggested that TNF-α/TNFRI interactions were central to PE_PGRS33-induced macrophage cell death.

Dheenadhayalan *et al.* (45) have reported that *M. smegmatis* expressing PE_PGRS33 elicits necrosis of murine bone marrow macrophages. Their studies and the results described in this study likely reflect distinct roles of PE_PGRS33 at different stages of infection. Dheenadhayalan *et al.* (45) addressed the role of PE_PGRS33 in the context of internalized bacteria residing in macrophages. The increased survival of the PE_PGRS33-expressing bacteria prompted the authors to suggest that necrosis of the host cell likely helps in persistence of the bacterium. Enhanced TNF-α release could only partially account for the observed effects. On the other hand, our studies unequivocally demonstrate that PE_PGRS33, a surface-exposed protein, interacts with TLR2 to elicit distinct effects on murine RAW 264.7 cells and human monocyte-derived macrophages, which are independent of internalization of the bacterium. The apoptotic effects of exogenous PE_PGRS33 or *M. smegmatis*-expressing PE_PGRS33 are entirely dependent on TNF-α. Recombinant 19-kDa lipoprotein has also been reported to induce macrophage apoptosis in a TLR2-dependent manner (46), suggesting that *M. tuberculosis* has a repertoire of modulins that signal through TLRs to effect apoptosis.

Our observations are of potential clinical significance considering that deletions in the PGRS domain of PE_PGRS33 alter the TNF-α-inducing properties of the protein. These studies offer important insight into how sequence variations in the polymorphic PGRS domain could modulate the immune response and thereby the course of infection.

Acknowledgments—We thank Prof. Jaya Tyagi for providing the genomic DNA of M. tuberculosis, Dr. Carsten Kirschning for the anti-TLR2 antibody, and Prof. Hidenori Ichijo and Prof. Roger Davis for plasmids.

REFERENCES

1. Stenger, S. (2005) *Ann. Rheum. Dis.* **64,** 24–28
2. Flynn, J. L., Goldstein, M. M., Chan, J., Triebold, K. J., Lowenstein, K., Schreiber, R., Mak, T. W., and Bloom, B. R. (1995) *Immunity* **2,** 561–572
3. Kindler, V., Sappino, A. P., Grau, G. E., Piguet, P. F., and Vassalli, P. (1989) *Cell* **56,** 731–740
4. Garcia, I., Miyazaki, Y., Marchal, G., Lesslauer, W., and Vassalli, P. (1997) *Eur. J. Immunol.* **27,** 3182–3190
5. Kaneko, H., Yamada, H., Mizuno, S., Udagawa, T., Kazumi, Y., Sekikawa, K., and Sugawara, I. (1999) *Lab. Investig.* **79,** 379–386
6. Bean, A. G. D., Roach, D. R., Briscoe, H., France, M. P., Korner, H., Sedgwick, J. D., and Britton, W. J. (1999) *J. Immunol.* **162,** 3504–3511
7. Ehlers, S., Benini, J., Kutsch, S., Endres, R., Rietschel, E. T., and Pfeffer, K. (1999) *Infect. Immun.* **67,** 3571–3579
8. Roach, D. R., Bean, A. G. D., Demangel, C., France, M. P., Briscoe, H., and Britton, W. J. (2002) *J. Immunol.* **168,** 4620–4627
9. Zganiacz, A., Santosuosso, M., Wang, J., Yang, T., Chen, L., Anzulovic, M., Alexander, S., Gicquel, B., Wan, Y., Bramson, J., Inman, M., and Xing, Z. (2004) *J. Clin. Investig.* **113,** 401–413
10. Gardam, M. A., Keystone, E. C., Menzies, R., Manners, S., Skamene, E., Long, R., and Vinh, D. C. (2003) *Lancet Infect. Dis.* **3,** 148–155
11. Mohan, A. K., Cote, T. R., Block, J. A., Manadan, A. M., Siegel, J. N., and Braun, M. M. (2004) *Clin. Infect. Dis.* **39,** 295–299
12. Keane, J., Gershon, S., Wise, R. P., Mirabile-Levens, E., Kasznica, J., Schwieterman, W. D., Siegal, J. N., and Brown, M. M. (2001) *N. Engl. J. Med.* **345,** 1098–1104
13. Leemans, J. C., Thepen, T., Weijer, S., Florquin, S., van Rooijen, N., van de Winkel, J. G., and van der Poll, T. (2005) *J. Infect. Dis.* **191,** 65–74
14. Winau, F., Weber, S., Sad, S., de Diego, J., Hoops, S. L., Breiden, B., Sandhoff, K., Brinkmann, V., Kaufmann, S. H. E., and Schaible, U. E. (2006) *Immunity* **24,** 105–117
15. Balcewicz-Sablinska, M. K., Keane, J., Kornfeld, H., and Remold, H. G. (1998) *J. Immunol.* **161,** 2636–2641
16. Rojas, M., Olivier, M., Gros, P., Barrera, L. F., and García, L. F. (1999) *J. Immunol.* **162,** 6122–6131
17. Cole, S. T., Brosch, R., Parkhill, J., Garnier, T., Churcher, C., Harris, D., Gordon, S. V., Eiglmeier, K., Gas, S., Barry, C. E., III, Tekaia, F., Badcock, K., Basham, D., Brown, D., Chillingworth, T., Connor, R., Davies, R., Devlin, K., Feltwell, T., Gentles, S., Hamlin, N., Holroyd, S., Hornsby, T., Jagels, K., Krogh, A., McLean, J., Moule, S., Murphy, L., Oliver, K., Osborne, J., Quail, M. A., Rajandream, M. A., Rogers, J., Rutter, S., Seeger, K., Skelton, J., Squares, R., Squares, S., Sulston, J. E., Taylor, K., Whitehead, S., and Barrell, B. G. (1998) *Nature* **393,** 537–544
18. Brennan, M. J., Delogu, G., Chen, Y., Bardarov, S., Kriakov, J., Alavi, M., and Jacobs, W. R., Jr. (2001) *Infect. Immun.* **69,** 7326–7333
19. Sampson, S. L., Lukey, P., Warren, R. M., van Helden, P. D., Richardson, M., and Everett, M. J. (2001) *Tuberculosis* **81,** 305–317
20. Delogu, G., Pusceddu, C., Bua, A., Fadda, G., Brennan, M. J., and Zanetti, S. (2004) *Mol. Microbiol.* **52,** 725–733
21. Ramakrishnan, L., Federspiel, N. A., and Falkow, S. (2000) *Science* **288,** 1436–1439
22. Voskuil, M. I., Schnappinger, S., Rutherford, R., Liu, Y., and Schoolnik, G. K. (2004) *Tuberculosis* **84,** 256–262
23. Akira, S., and Takeda, K. (2004) *Nat. Rev. Immunol.* **4,** 499–511
24. Drennan, M. B., Nicolle, D., Quesniaux, V. J., Jacobs, M., Allie, N., Mpagi, J., Fremond, C., Wagner, H., Kirschning, C., and Ryffel, B. (2004) *Am. J. Pathol.* **164,** 49–57
25. Reiling, N., Holscher, C., Fehrenbach, A., Kroger, S., Kirschning, C., Goyert, S., and Ehlers, S. (2002) *J. Immunol.* **169,** 3480–3484
26. Talarico, S., Cave, M. D., Marrs, C. F., Foxman, B., Zhang, L., and Yang, Z. (2005) *J. Clin. Microbiol.* **43,** 4954–4960
27. Pathak, S. K., Bhattacharyya, A., Pathak, S., Basak, C., Mandal, D., Kundu, M., and Basu, J. (2004) *J. Biol. Chem.* **279,** 55127–55136
28. Choudhuri, B. S., Bhakta, S., Barik, R., Basu, J., Kundu, M., and Chakrabarti, P. (2002) *Biochem. J.* **367,** 279–285
29. Goddette, D. W., and Frieden, C. (1986)) *J. Biol. Chem.* **261,** 15974–15980
30. Manor, E., and Sarov, I. (1986) *Infect. Immun.* **54,** 90–95
31. Bhattacharyya, A., Pathak, S., Basak, C., Law, S., Kundu, M., and Basu, J. (2003) *J. Biol. Chem.* **278**, 26517–26525
32. Krippner, A., Matsuno-Yagi, A., Gottlieb, R. A., and Babior, B. M. (1996) *J. Biol. Chem.* **271,** 21629–21636
33. Ichijo, H., Nishida, E., Irie, N., den Dijke, P., Saitoh, M., Moriguchi, T., Takagi, M., Matsumoto, K., Miyazono, K., and Gotoh, Y. (1997) *Science* **275**, 90–94
34. Nishitoh, H., Saitoh, M., Mochida, Y., Takeda, K., Nakano, H., Rothe, M., Miyazono, K., and Ichijo, H. (1998) *Mol. Cell* **2**, 389–395
35. Tobiume, K., Matsuzawa, A., Takahashi, T., Nishitoh, H., Morita, K.-I., Takeda, K., Minowa, O., Miyazono, K., Noda, T., and Ichijo, H. (2001) *EMBO Rep.* **2,** 222–228
36. Into, T., and Shibata, K. (2005) *Cell. Microbiol.* **7,** 1305–1317
37. Aliprantis, A. O., Yang, R. B., Weiss, D. S., Godowski, P., and Zychlinsky, A. (2000) *EMBO J.* **19,** 3325–3326
38. Wang, X. (2001) *Genes Dev.* **15,** 2922–2933
39. Gross, A., Yin, X. M., Wang, K., Wei, M. C., Jockel, J., Milliman, C., Erdjument-Bromage, H., Tempst, P., and Korsmeyer, S. J. (1999) *J. Biol. Chem.* **274,** 1156–1163
40. Wang, K., Yin, X. M., Chao, D. T., Milliman, C. L., and Korsmeyer, S. J. (1996) *Genes Dev.* **10**, 2859–2869
41. Rahman, M. M., and McFadden, G. (2006) *Plos Pathogens* **2,** 66–77
42. Banu, S., Honore, N., Saint-Joanis, B., Philpott, D., Prevost, M.-C., and Cole, S. T. (2002) *Mol. Microbiol.* **44,** 9–19
43. van Soolingen, D. M., de Haas, P. E. W., Hermans, P. W. M., Groenen, P. M. A., and van Embden, J. D. A. (1993) *J. Clin. Microbiol.* **31,** 1987–1995
44. Yang, C.-S., Song, C.-H., Lee, J.-S., Jung, S.-B., Oh, J.-H., Park, J., Kim, H.-J., Park, J.-K., Paik, T.-H., and Jo, E.-K. (2006) *Cell. Microbiol.* **8,** 1158–1171
45. Dheenadhayalan, V., Delogu, G., and Brennan, M. J. (2006) *Microbes Infect.* **8,** 262–272
46. Lopez, M., Sly, L. M., Luu, Y., Young, D., Cooper, H., and Reiner, N. E. (2003) *J. Immunol.* **170,** 2409–2416